Electronic Supporting Information

Supramolecular 3d-4f Single-Molecule Magnet Architecture

Sebastian Schmitz,[a] Jan van Leusen,[a] Natalya V. Izarova,[b] Yanhua Lan,[c] Wolfgang Wernsdorfer,[c,d,e] Paul Kögerler,*[a,b] and Kirill Yu. Monakhov*[a]

[a] Institut für Anorganische Chemie, RWTH Aachen University, Landoltweg 1, 52074 Aachen (Germany).

[b] Jülich-Aachen Research Alliance (JARA-FIT) and Peter Grünberg Institute (PGI-6), Forschungszentrum Jülich, 52425 Jülich (Germany).

[c] Institut Néel (CNRS/UJF UPR2940), 25 rue des Martyrs BP 166, 38042 Grenoble cedex 9 (France).

[d] Physikalisches Institut, Karlsruhe Institute of Technology (KIT), Wolfgang-Gaede-Str. 1, D-76131 Karlsruhe (Germany).

[e] Institut für Nanotechnologie, Karlsruhe Institute of Technology (KIT), Hermann-von-Helmholtz-Platz 1, D-76344 Eggenstein-Leopoldshafen (Germany).

Contents:

1. Synthesis and characterization of compounds 1–3

Materials and methods

The syntheses were carried out under aerobic conditions. All starting materials were from commercial sources and were used as received. Solvents were used without further purification. The IR spectra were recorded on a Nicolet Avatar 360 FTIR spectrometer (KBr pellets, ν = 4000–400 cm^{-1}). The ESI-MS spectra in the negative ion mode were recorded on a 4000 QTRAP mass spectrometer system, using the LC/LC-MS method with direct infusion.

Compound 1

{[$Dy(OAc)_3(H_2O)_3$][$Dy(H_2O)_3(prop{\cdot}SMe)_3$][$H_2O\subset Cr_3Dy_6(OAc)_{12}(H_2bda)_3(glyc)_3(ox)_3(prop{\cdot}SMe)_3$]$_2$ (H_2O)}$\cdot 12H_2O\cdot 1.5MeCN$

3-(methylthio)propionic acid (0.116 mL; 1.12 mmol) and *N*-butyldiethanolamine (0.170 mL; 1.02 mmol) were added to the mixture of [$Cr_3(OH)_2(OAc)_7$] (0.100 g; 0.17 mmol) and $Dy(OAc)_3{\cdot}4H_2O$ (0.206 g; 0.50 mmol) in 7 mL of MeCN. The reaction mixture was stirred for 2 h under reflux, resulting in the color change from cloudy green to clear violet. The MeCN solution was filtered off and the filtrate was kept in a capped vial at room temperature. Pink single crystals suitable for X-ray diffraction were obtained via slow evaporation after *ca.* two weeks. Yield: 0.013 g (4.8 % based on Dy; $C_{165}H_{322.5}Cr_6Dy_{14}N_{7.5}O_{147}S_9$, 7639.34 g mol^{-1}).

IR (KBr pellet), ν_{max} / cm^{-1}: 3412 (br, s), 3191 (sh), 2963 (m), 2922 (sh), 2872 (sh), 1668 (s) 1573 (s), 1414 (s), 1314 (w), 1154 (vw), 1101 (w), 1057 (m), 1023 (sh), 937 (w, sh), 918 (m), 795 (w), 751 (w), 674 (m), 608 (w), 541 (vw), 484(w).

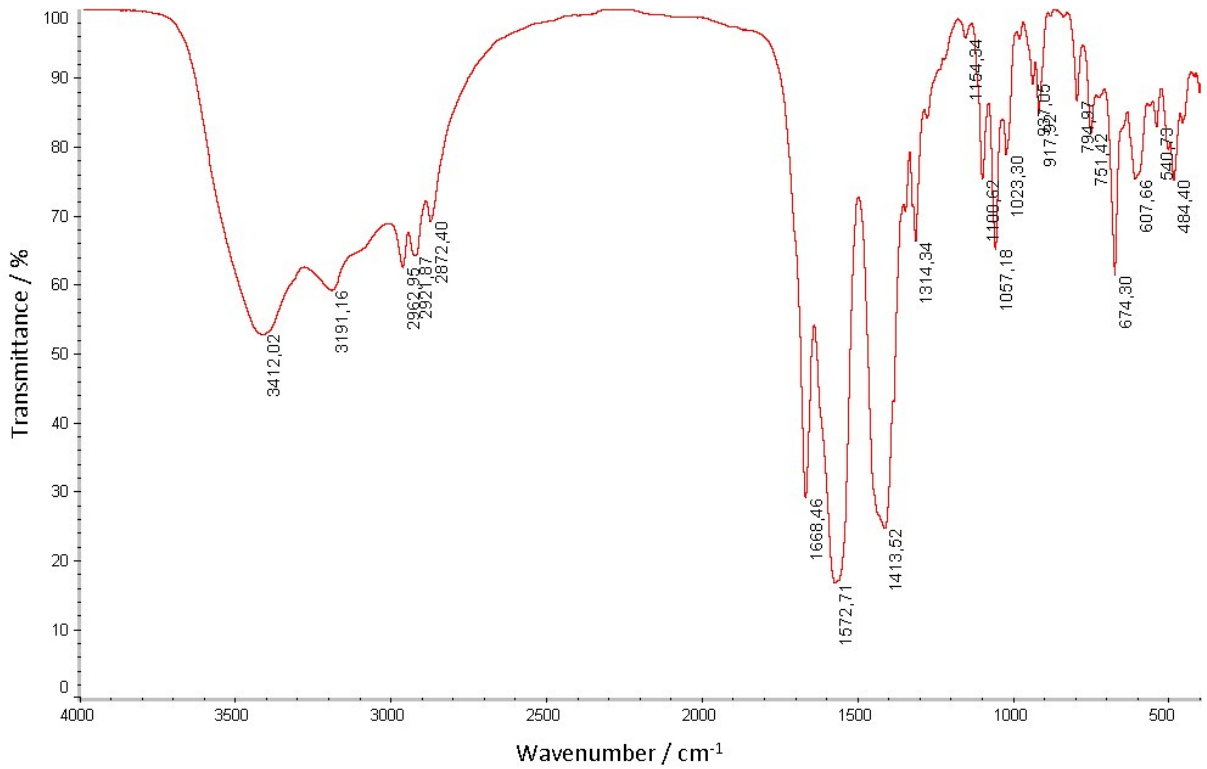

Figure S1: IR spectrum of compound **1** in the 4000–400 cm^{-1} region (KBr pellet).

Compound 2

{[Tb(OAc)$_3$(H$_2$O)$_3$][Tb(H$_2$O)$_3$(prop·SMe)$_3$][H$_2$O⊂Cr$_3$Tb$_6$(OAc)$_{12}$(H$_2$bda)$_3$(glyc)$_3$(ox)$_3$(prop·SMe)$_3$]$_2$(H$_2$O)}·11.25H$_2$O·1.5 MeCN

Compound **2** was prepared following the protocol for synthesis of compound **1**, by using Tb(OAc)$_3$·4H$_2$O (0.205 g; 0.50 mmol) instead of Dy(OAc)$_3$·4H$_2$O. Pink single crystals suitable for X-ray diffraction were obtained via slow evaporation after *ca.* two weeks. Yield: 0.012 g (4.4 % based on Tb; $C_{165}H_{321}Cr_6N_{7.5}O_{146.25}S_9Tb_{14}$, 7575.78 g mol^{-1}). Sulfur content according to elemental analysis: calcd. 3.95 % (disregarding solvent), found 4.3 % (deviation ± 0.2%).

IR (KBr pellet), ν_{max} / cm^{-1}: 3407 (br, m), 3189 (br, m), 2962 (m), 2920 (sh), 2872 (sh), 1668 (s), 1575 (s), 1413 (s), 1346 (w, sh), 1313 (m), 1277 (vw), 1154 (w), 1101 (m), 1055 (m), 1022 (w, sh), 936 (w, sh), 917 (m), 793 (m), 750 (m), 673 (m), 606 (m), 540 (w), 483 (m), 456 (vw, sh).

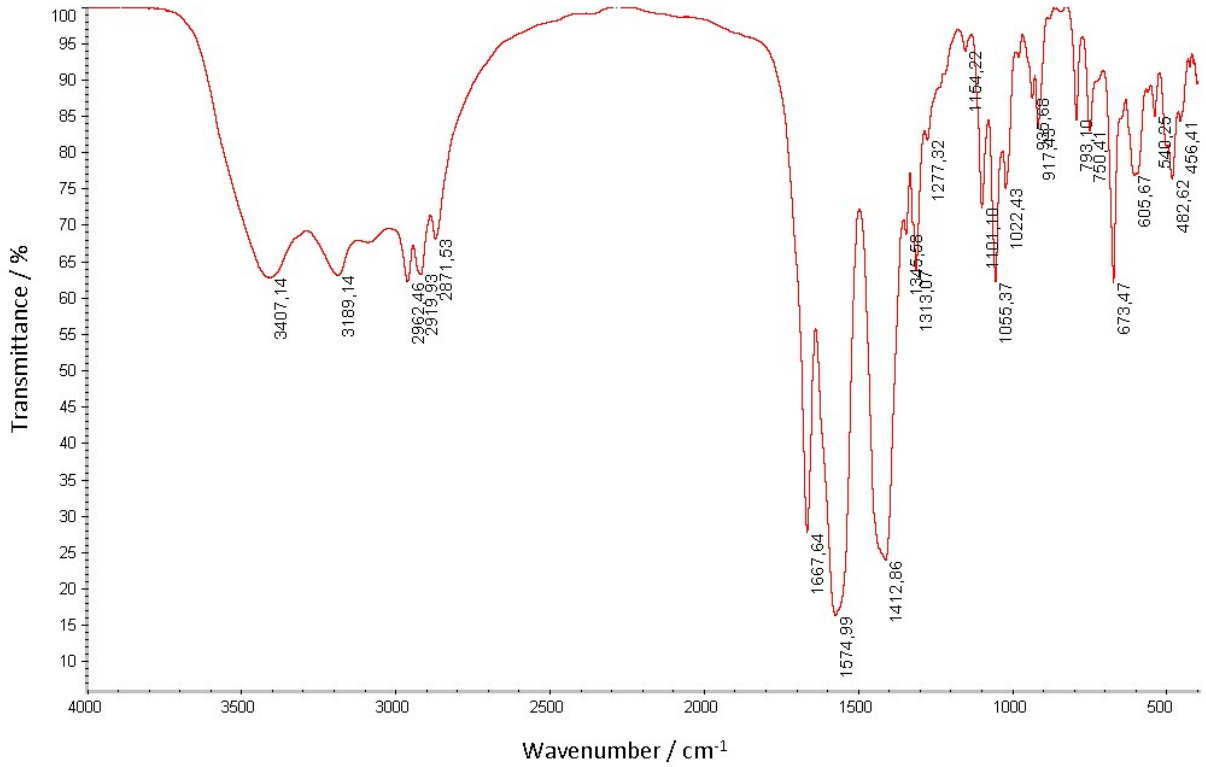

Figure S2: IR spectrum of compound **2** in the 4000–400 cm^{-1} region (KBr pellet).

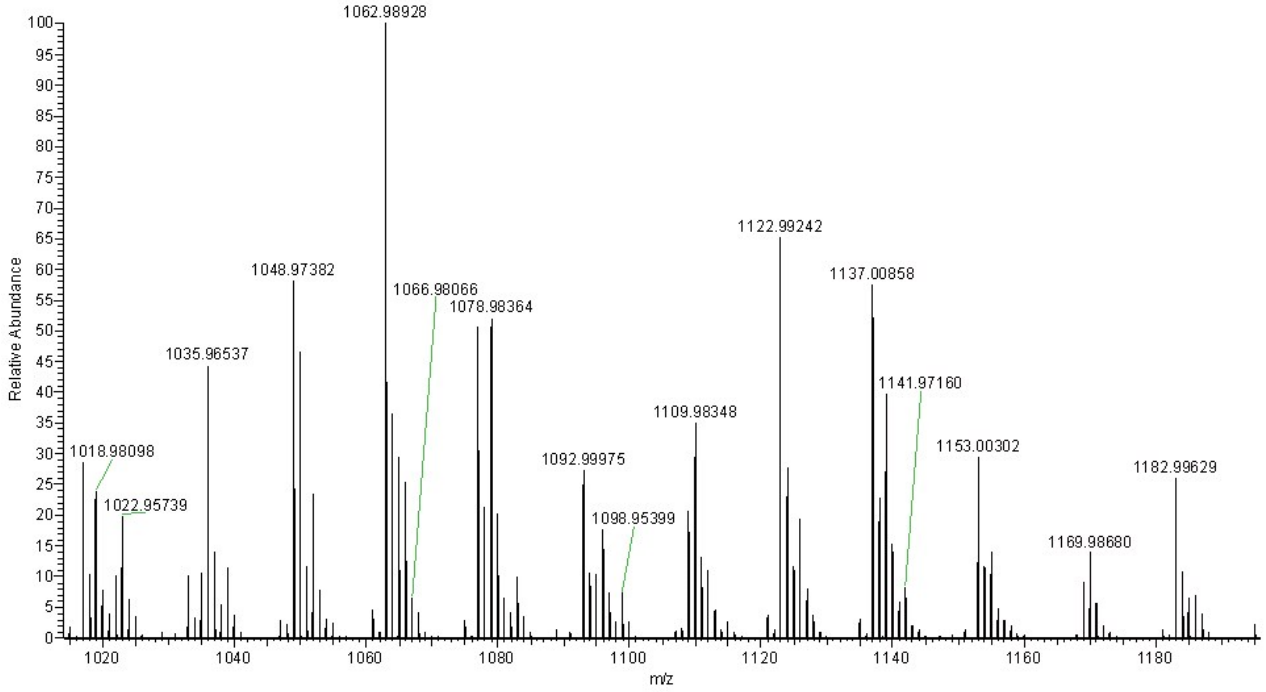

Figure S3: ESI-MS spectrum of compound **2**. The experimental molecular ion peak of $[CrTb_2(OAc)_3(prop{\cdot}SMe)(H_2bda)(glyc)_3]^-$ is 100 %. For more details, see Table S1.

Table S1: ESI-MS data for compound **2**.

Measured [Da]	Calculated [Da]	Sum formula	Composition
1062.98928	1063.0067	$(Cr_1Tb_2C_{25}H_{43}O_{19}N_1S_1)^-$ 100 %	$[CrTb_2(OAc)_3(\mathbf{prop{\cdot}SMe})(H_2bda)(glyc)_3]^-$
1122.99242	1123.0279	$(Cr_1Tb_2C_{27}H_{47}O_{21}N_1S_1)^-$ 60 %	$[CrTb_2(OAc)_4(\mathbf{prop{\cdot}SMe})(H_2bda)(Hglyc)(glyc)_2]^-$
1048.97382	1048.9547	$(Cr_1Tb_2C_{23}H_{37}O_{20}N_1S_1)^-$ 60 %	$[CrTb_2(\mathbf{prop{\cdot}SMe})(H_2bda)(Hglyc)(glyc)_3(ox)]^-$
1137.00858	1136.9344	$(Cr_1Tb_2C_{25}H_{37}O_{24}N_1S_1)^-$ 58 %	$[CrTb_2(OAc)(\mathbf{prop{\cdot}SMe})(H_2bda)(Hglyc)_2(ox)_3]^-$
1153.00302	1152.9293	$(Cr_1Tb_2C_{25}H_{37}O_{25}N_1S_1)^-$ 30 %	$[CrTb_2(\mathbf{prop{\cdot}SMe})(H_2bda)(Hglyc)_3(ox)_3]^-$
1018.98098	1018.9805	$(Cr_1Tb_2C_{23}H_{39}O_{18}N_1S_1)^-$ 29 %	$[CrTb_2(OAc)(\mathbf{prop{\cdot}SMe})(H_2bda)(glyc)_4]^-$
1182.99629	1182.9762	$(Cr_1Tb_2C_{27}H_{43}O_{25}N_1S_1)^-$ 25 %	$[CrTb_2(OAc)_2(\mathbf{prop{\cdot}SMe})(H_2bda)(Hglyc)_3(ox)_2]^-$

Compound 3

$[Tb(OAc)_3(H_2O)_3]_2[Cr_3Tb_6(OAc)_{15}(H_2bda)_3(glyc)_3(ox)_3]_2{\cdot}13.5H_2O{\cdot}1.5MeCN$

4-(methylthio)phenol (0.140 g; 1.0 mmol) and *N*-butyldiethanolamine (0.170 mL; 1.02 mmol) were added to the mixture of $[Cr_3(OH)_2(OAc)_7]$ (0.100 g; 0.17 mmol) and $Tb(OAc)_3{\cdot}4H_2O$ (0.205 g; 0.50 mmol) in 7 mL of MeCN. The reaction mixture was stirred for 2 h under reflux, resulting in the color change from cloudy green to clear violet. The MeCN solution was filtered off and the filtrate was kept in a capped vial at room temperature. Pink single crystals suitable for X-ray diffraction were obtained via slow evaporation after *ca.* two weeks. Yield: 0.007 g (2.8 % based on Tb; $C_{147}H_{283.5}Cr_6N_{7.5}O_{145.5}Tb_{14}$, 7021.19 g mol^{-1}).

IR (KBr pellet), ν_{max} / cm^{-1}: 3423 (br, m), 2963 (m), 2930 (sh), 2872 (sh), 1668 (s), 1571 (s), 1497 (w), 1417 (s), 1346 (w, sh), 1314 (m), 1269 (vw), 1154 (w), 1101 (m), 1056 (m), 1023 (w, sh), 937 (w, sh), 917 (m), 794 (m), 750 (m), 674 (m), 594 (m), 540 (w), 483 (m).

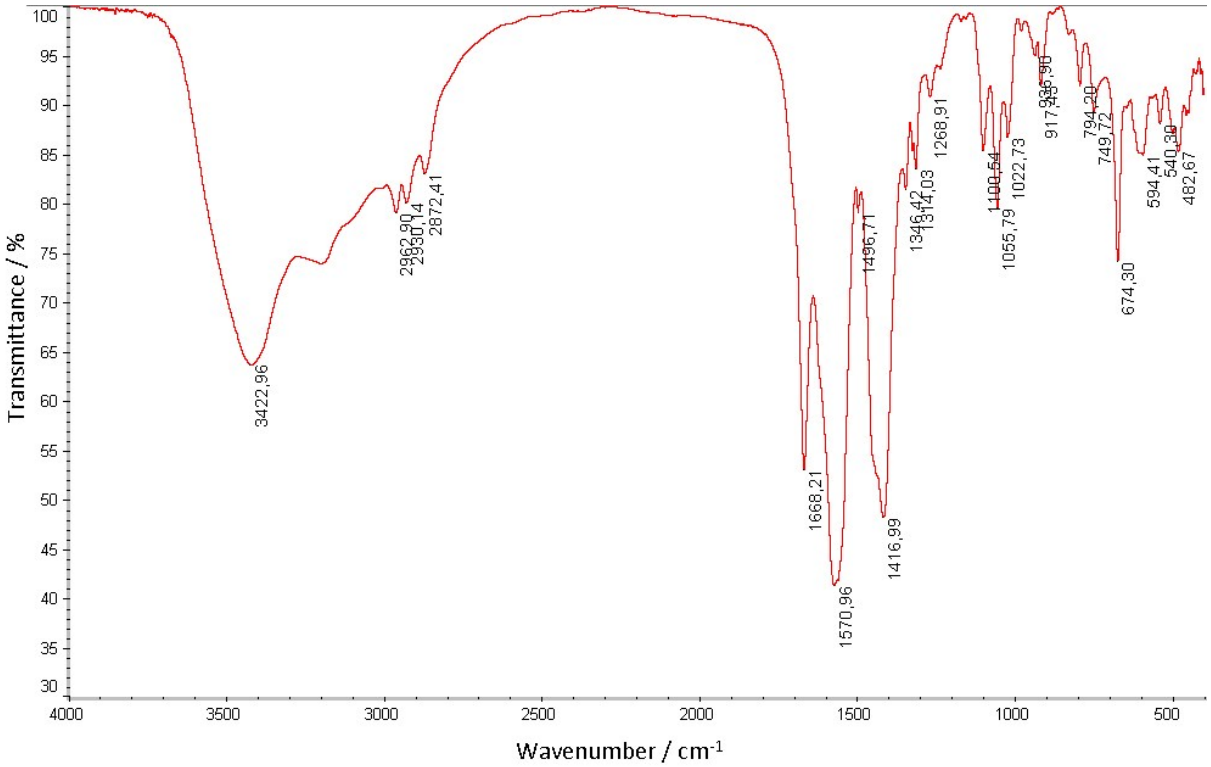

Figure S4: IR spectrum of compound **3** in the 4000–400 cm^{-1} region (KBr pellet).

Experiments probing the direct addition of oxalates and glycolates to the reaction solutions

Upon addition of small amounts of oxalic and glycolic acids to the reaction mixtures, no crystalline product could be isolated. In this situation the reaction mixtures show a color change from cloudy green to cloudy violet. We observed that the use of a larger amounts of the oxalic (0.17–0.70 mmol) and glycolic (0.17–0.70 mmol) acids leads to less cloudy mixtures; however, the latter exhibit a more bluish color than the reaction mixtures obtained in the synthesis of **1** and **2**.

2. Crystal data and structure refinement details for compounds 1–3

X-ray Crystallography

Single-crystal diffraction data for compounds **1–3** were collected on a SuperNova (Agilent Technologies) diffractometer with MoKα radiation (λ = 0.71073 Å) at 120 K. The crystals were mounted in a Hampton cryoloop with Paratone-N oil to prevent water loss. Absorption corrections were applied numerically based on multifaceted crystal model using CrysAlis software.[1] The SHELXTL software package[2] was used to solve and refine the structure. The structures were solved by direct methods and refined by full-matrix least-squares method against $|F|^2$ with anisotropic thermal parameters for all atoms besides hydrogens for compound **3** and all atoms besides hydrogens as well as C, S and O atoms of heavily disordered $–CH_2–S–CH_3$ moieties of SMe·prop ligands and solvent water molecules for compounds **1** and **2**. Due to disorder the positions of some $–CH_3$ groups in $–CH_2–S–CH_3$ moieties could not be determined or the sum of occupancies of located positions for $–S–CH_3$ fragments of the same moieties were lower than that for $–CH_2–$ groups. In this case the exact number of SMe·prop ligands was calculated by the occupancy of $–CH_2–$ groups and included to the formula. The hydrogen atoms of the crystal waters, $–CH_2–S–CH_3$ moieties of SMe·prop as well as OH groups of glyc and H_2bda ligands were not located. All the other hydrogen atoms were placed in geometrically calculated positions. The relative site occupancy factors for the disordered positions of carbon and sulfur atoms of $–CH_2–S–CH_3$ moieties as well as oxygen, carbon and nitrogen atoms of co-crystallized solvent water and acetonitrile molecules were first refined in an isotropic approximation with U_{iso}= 0.05 and then fixed at the obtained values and refined without the thermal parameters restrictions. DELU restrictions had to be applied to some carbon atoms of the H_2bda ligands as well as C and O atoms of acetate groups.

The formal oxidation states of Cr and Ln ions were established by bond valence sum analysis: $\Sigma_{bv}(Cr^{III})$ = 2.80 – 2.94 and $\Sigma_{bv}(Dy^{III})$ = 2.83 – 3.17 for **1**; $\Sigma_{bv}(Cr^{III})$ = 2.91 – 3.04 and $\Sigma_{bv}(Tb^{III})$ = 2.81 – 3.08 for **2**.

Additional crystallographic data are summarized in Table S2. Further details on the crystal structures investigation can be obtained, free of charge, on application to CCDC, 12 Union Road, Cambridge CB2 1EZ, UK: http://www.ccdc.cam.ac.uk/, e-mail: data_request@ccdc.cam.ac.uk, or fax: +441223 336033 upon quoting 1487793 (**1**), 1487794 (**2**) and 1487795 (**3**) numbers.

Table S2: Crystallographic details for compounds **1–3**

Sample	**1**	**2**	**3**
Empirical formula (XRD) *	$C_{153.9}H_{271.8}Cr_6Dy_{14}N_{7.5}O_{147}S_{4.95}$	$C_{156}H_{302.5}Cr_6N_{7.5}O_{146.25}S_{4.5}Tb_{14}$	$C_{147}H_{283.5}Cr_6N_{7.5}O_{145.5}Tb_{14}$
Formula weight, g/mol	7325.09	7300.70	7021.19
"Disorder-corrected formula" **	$C_{165}H_{322.5}Cr_6Dy_{14}N_{7.5}O_{147}S_9$	$C_{165}H_{321}Cr_6N_{7.5}O_{146.25}S_9Tb_{14}$	$C_{147}H_{283.5}Cr_6N_{7.5}O_{145.5}Tb_{14}$
Crystal system	Trigonal	Trigonal	Trigonal
Space group	*P*31*c*	*P*31*c*	*P*31*c*
a / Å	23.9817(4)	24.0037(6)	23.7804(3)
c / Å	31.9326(4)	32.0420(9)	31.8903(3)
V / Å^3	15904.7(4)	15988.5(7)	15618.0(3)
Z	2	2	2
D_{calc} / g cm^{-3}	1.530	1.517	1.493
Absorption coefficient / mm^{-1}	3.553	3.357	3.404
F(000)	7142	7174	6872
Crystal size / mm	0.22× 0.29 × 0.39	0.15 × 0.18 × 0.22	0.22 × 0.35 × 0.48
Theta range for data collection	4.11° – 24.41°	4.10° – 24.40°	4.13° – 26.37°
Completeness to Θ_{max}	99.5%	99.5%	99.6%
Index ranges	$-27 \le h \le 27$, $-27 \le k \le 27$, $-36 \le l \le 37$	$-27 \le h \le 24$, $-27 \le k \le 24$, $-37 \le l \le 37$	$-28 \le h \le 29$, $-29 \le k \le 29$, $-39 \le l \le 39$
Reflections collected	92526	73946	105211
Independent reflections	17367	17388	21210
R_{int}	0.0893	0.1168	0.0784
Observed ($I > 2\sigma(I)$)	12219	11562	15192
Absorption correction	Analytical using a multifaceted crystal model		
T_{min} / T_{max}	0.2905 / 0.5109	0.5480 / 0.6271	0.2535 / 0.5223
Data / restraints / parameters	17367 / 51 / 1058	17388 / 55 / 1039	21210 / 42 / 989
Goodness-of-fit on F^2	1.091	1.054	1.071
R_1, wR_2 ($I > 2\sigma(I)$)	R_1 = 0.0865, wR_2 = 0.2054	R_1 = 0.0708, wR_2 = 0.1569	R_1 = 0.0640, wR_2 = 0.1507
R_1, wR_2 (all data)	R_1 = 0.1314, wR_2 = 0.2467	R_1 = 0.1236, wR_2 = 0.1871	R_1 = 0.1070, wR_2 = 0.1819
Largest diff. peak and hole, e. Å^{-3}	4.421 and –1.046	2.131 and –0.809	1.546 and –1.498

Photograph of a characteristic crystal of compounds 1 and 2 coated with Paratone-N oil

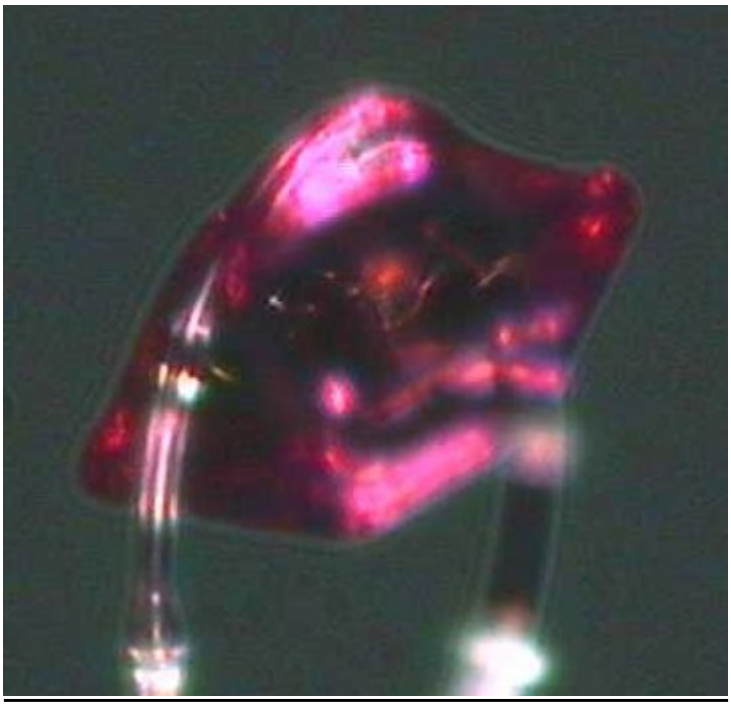

Solid-state packing

In the crystal lattices of compounds **1** and **2**, the $\{Cr_6Ln_{14}\}$ aggregates are packed to yield a honeycomb structure in the *ab* plane:

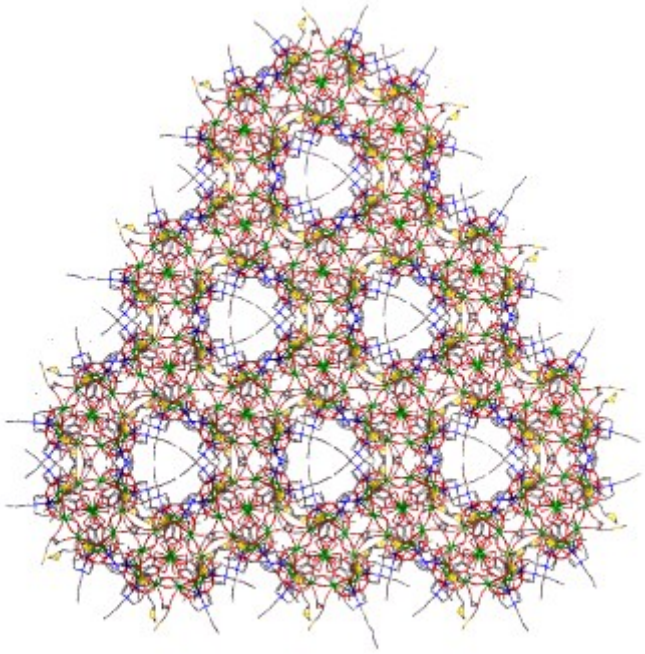

3. Survey of metal-ligand coordination modes

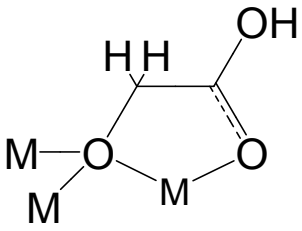

0 hits in database
M = any metal

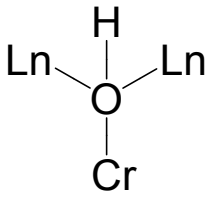

Ln = Tb: 3 hits in database
Ln = Dy: 4 hits in database

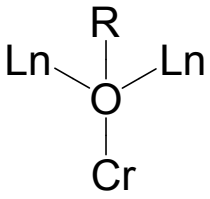

Ln = Tb: 0 hits
Ln = Dy: 4 hits, R = Me

4. Depiction of used and obtained ligands in the synthesis of compounds 1–3

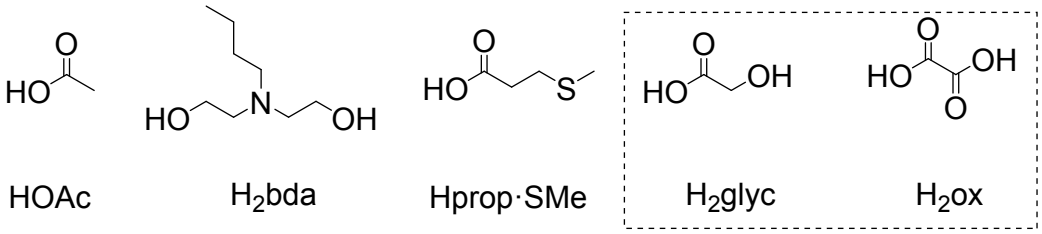

added ligands ***in situ*** **formed ligands**

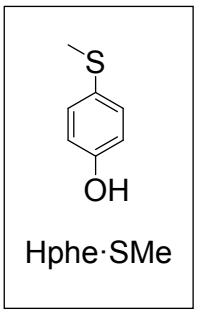

"crystallization reagent"

5. Magnetic properties of compounds 1 and 2

General methods

Magnetic data of compounds **1** and **2** were recorded using a Quantum Design MPMS-5XL SQUID magnetometer. The polycrystalline samples were compacted and immobilized into cylindrical PTFE capsules. DC data were acquired as a function of the magnetic field (0.1−5.0 T at 2.0 K) and temperature (2.0–290 K at 0.1 T). AC data were measured in the absence of a static bias field in the frequency range 1−1000 Hz (T = 2.0−50 K, B_{ac} = 3 G). Data were corrected for the diamagnetic contributions of sample holder and compound (**1:** χ_{dia} = -3.80×10^{-3} cm^3 mol^{-1}, **2:** χ_{dia} = -3.77×10^{-3} cm^3 mol^{-1}).

Supplementary ac susceptibility data for compound 1

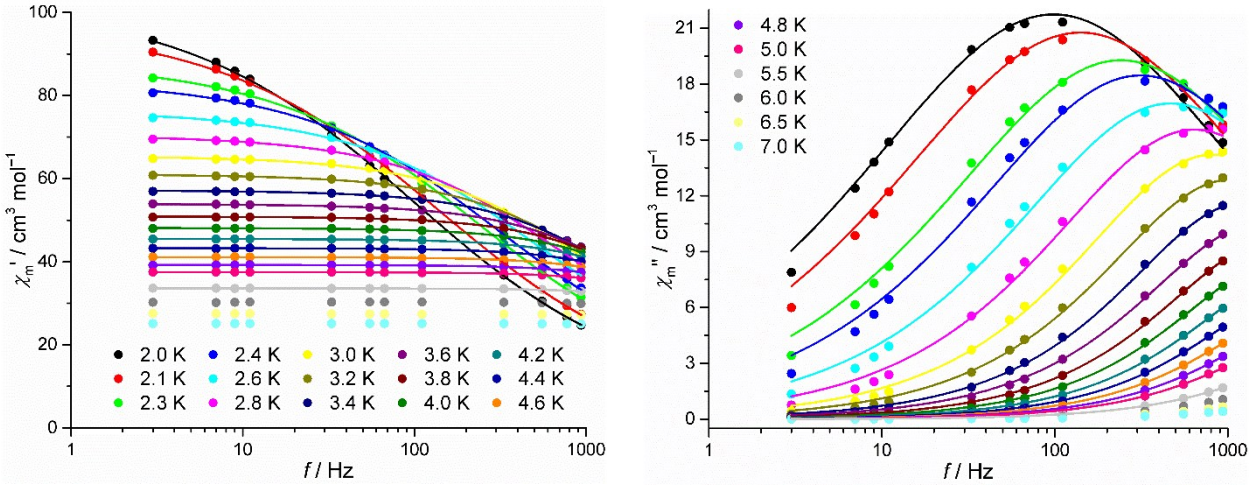

Figure S5: In-phase χ_m' and out-of-phase χ_m'' magnetic ac susceptibility versus frequency f at zero static bias field of compound **1**: experimental data (full dots); fit to generalized Debye expression[3] (solid lines).

Magnetic properties of compound 2

The magnetic dc data of compound **2** are depicted in Fig. S6 as χ_mT *vs*. T and M_m *vs*. B plots. The χ_mT value of 170.43 cm^3 K mol^{-1} at 290 K is slightly below the range 175–179.6 cm^3 K mol^{-1} expected[4] for six high-spin Cr^{III} and 14 Tb^{III} non-interacting centers. As for compound **1**, such a value hints at the presence of small intramolecular antiferromagnetic exchange interactions. By lowering temperature, the χ_mT value is almost constant until *ca*. 200 K, decreases to a minimum at

ca. 5.5 K, and subsequently increases to a maximum of 120.93 cm^3 K mol^{-1} at 2.2 K. The behavior in the range 5.5–290 K indicates antiferromagnetic interactions and/or the thermal depopulation of the m_J substates of the Tb^{III} centers while the increase at low temperatures hints at ferromagnetic exchange interactions. The molar magnetization M_m at 2.0 K is a linear function of the applied field B up to *ca*. 0.3 T, and is a straight line with a different slope for 2–5 T reaching 61.8 $N_A \mu_B$ at 5 T. This value is considerably below the saturation value of *ca*. 144 $N_A \mu_B$, and may be thus due to antiferromagnetic exchange interactions. However, since the curve is clearly rising at 5 T the small magnetization values may be also due to single-ion effects of the Tb^{III} centers. In summary, the magnetic dc data reveal antiferromagnetic and ferromagnetic exchange interactions within the compound besides single-ion effects.

The ac magnetic susceptibility data at zero bias field show slow relaxation for temperatures below 4.6 K within the limits of the experimental set-up (see Figs. S7 and S8). Analyzing the in-phase χ_m' and out-of-phase χ_m'' components as a function of the applied frequency f in terms of a generalized Debye expression[3] yields least-squares fits which are depicted as solid lines in Figs. S7 and S8. The distribution of relaxation times α suggest the existence of multiple relaxation pathways (0.12-0.32, mean 0.22), and the semi-logarithmic representation of τ *vs.* T^{-1} indicates a mono-exponential relation. Fitting the data thus to a single Arrhenius expression $\tau = \tau_0 \cdot \exp[U_{eff}/(k_B T)]$ in the range 2.0-3.4 K (see Fig. S8) yields the attempt time $\tau_0 = (7.5\pm0.8)\times10^{-6}$ s and the effective energy barrier $U_{eff} = (3.4\pm0.2)$ cm^{-1} representing a rather large Orbach relaxation time and a small effective energy barrier.[5]

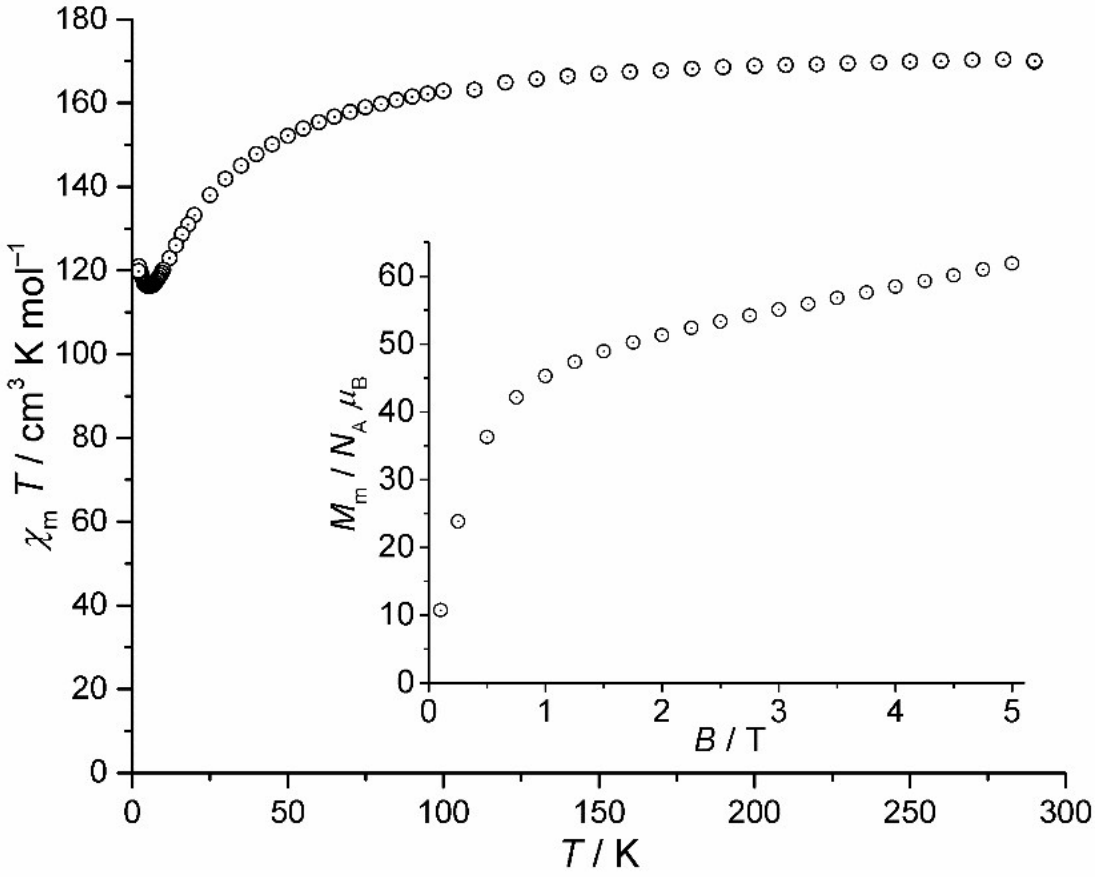

Figure S6: Temperature dependence of $\chi_m T$ at 0.1 T of compound **2**; inset: molar magnetization M_m versus applied field B at 2.0 K.

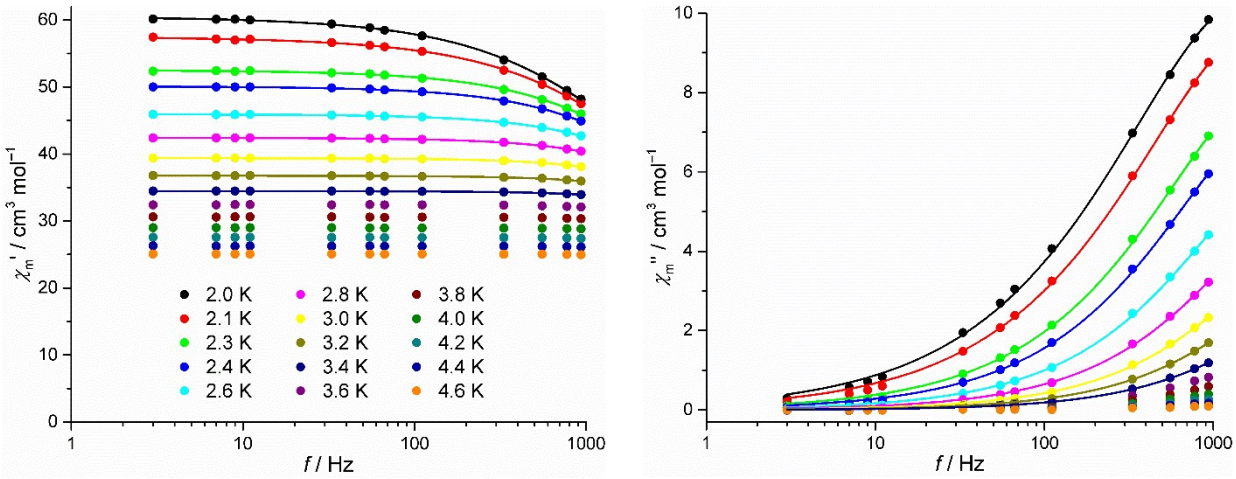

Figure S7: In-phase χ_m′ and out-of-phase χ_m″ magnetic ac susceptibility versus frequency f at zero static bias field of compoud **2**: experimental data (full circles); fit to generalized Debye expression[3] (solid lines).

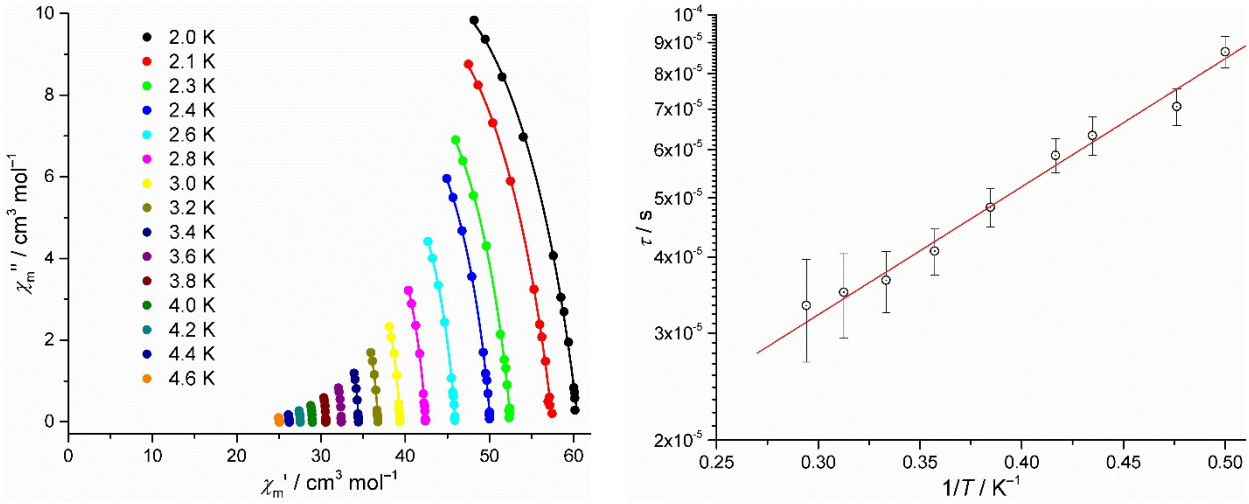

Figure S8: Left: Cole-Cole plot of compound **2**: experimental data (full circles); fit to generalized Debye expression[3] (solid lines). Right: Arrhenius plot of relaxation time τ vs. T^{-1} (2.0 K ≤ T ≤ 3.4 K) of compound **2** (open circles); solid line shows fit to Arrhenius expression.

Low-temperature micro-SQUID measurements

Low-temperature magnetization measurements were carried out on single crystals with a home-built array of micro-SQUIDs between 0.03–5 K using an applied field with sweep rates of 0.001–0.280 T/s. The magnetization measurements were performed with the magnetic applied field aligned parallel to the easy axis of magnetization by using the transverse field method. The field is applied in any direction of the micro-SQUID plane with precision greater than 0.1° by separately driving three orthogonal coils.[6]

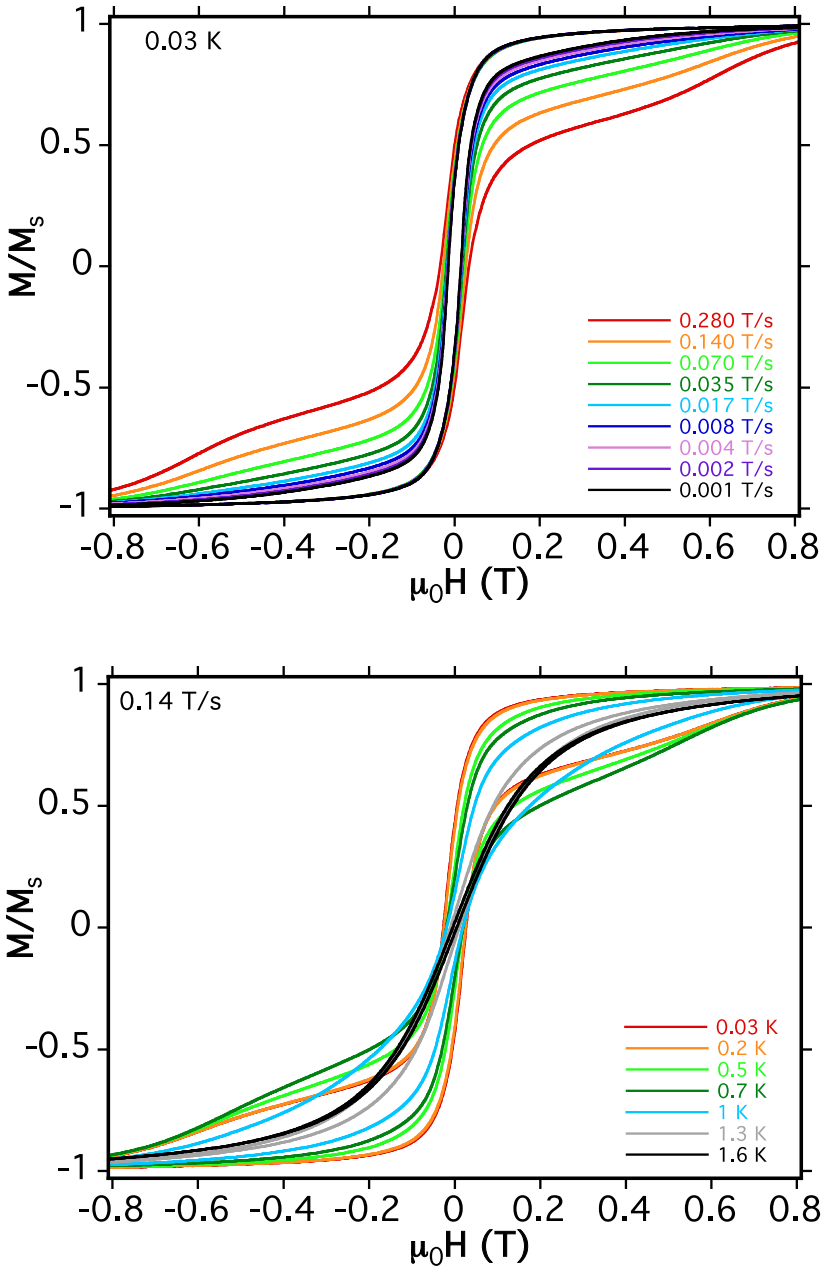

Figure S9: Sweep rate dependence (top) and temperature dependence (bottom) of magnetization curves measured as a function of an applied magnetic field at 0.03 K and at a sweeping rate of 0.14 T/s for **1**. The magnetization is normalized to its saturation value M_s at 1.4 T.

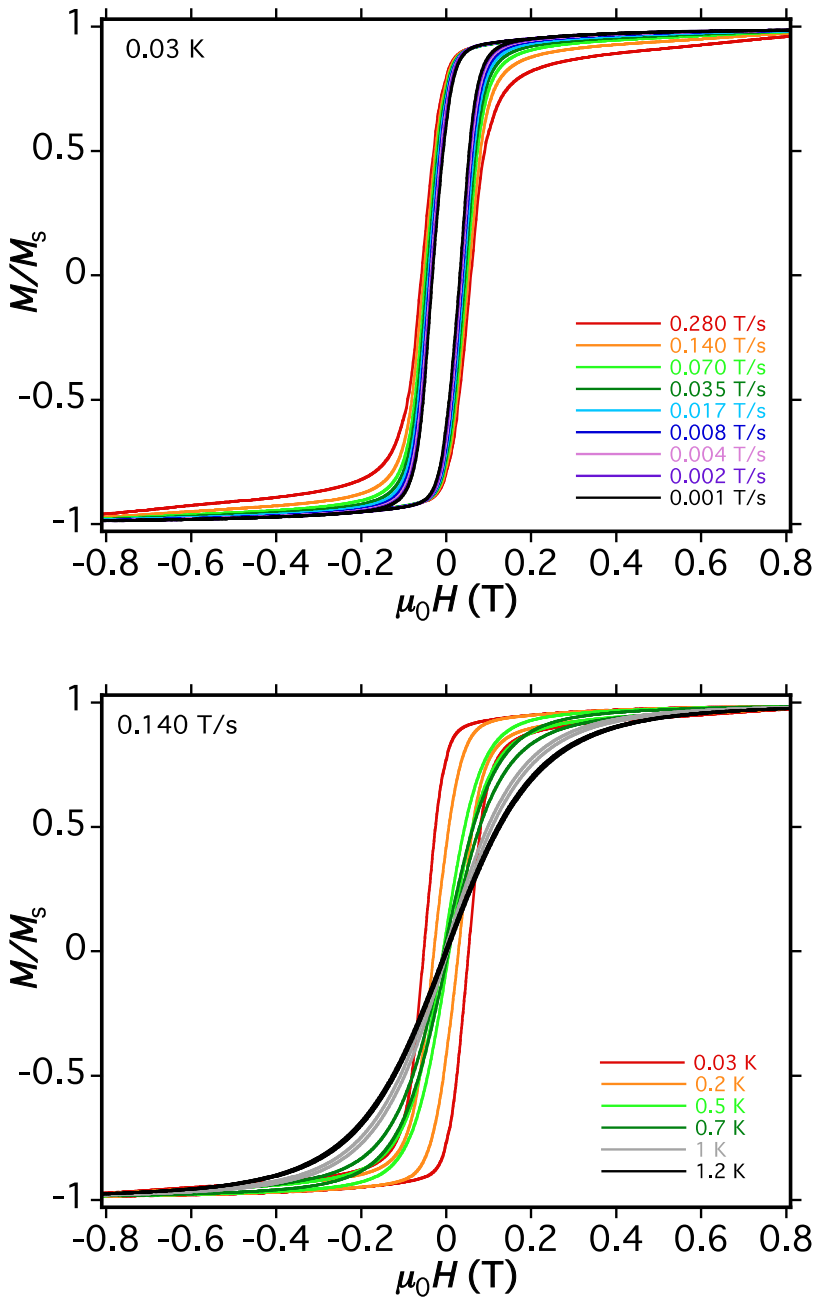

Figure S10: Sweep rate dependence (top) and temperature dependence (bottom) of magnetization curves measured as a function of the applied magnetic field at 0.03 K and at a sweeping rate of 0.14 T/s for **2**. The magnetization is normalized to its saturation value M_s at 1.4 T.

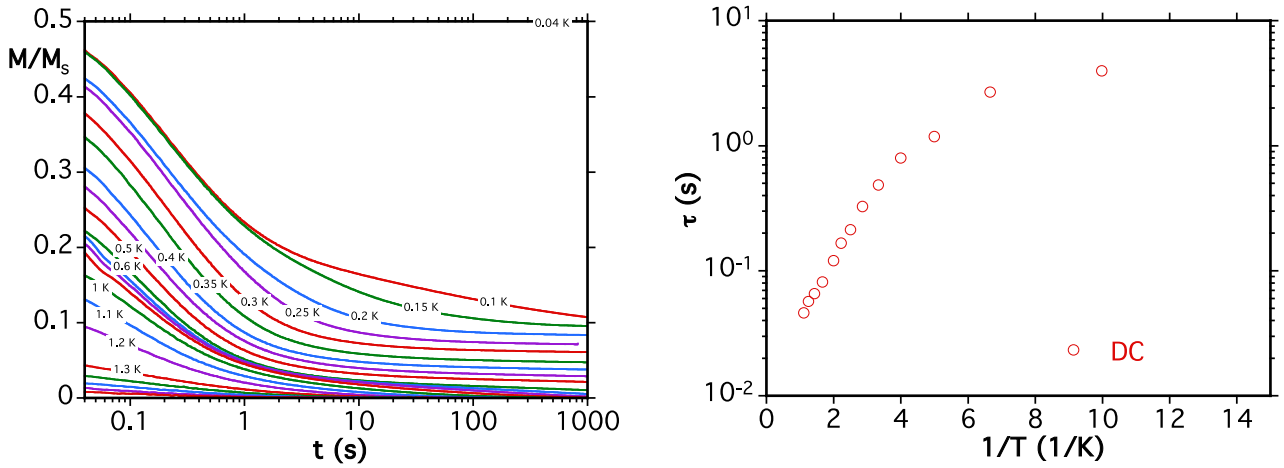

Figure S11: Magnetization decay measurements for compound **1** at the indicated temperatures (left) and relaxation time (right).

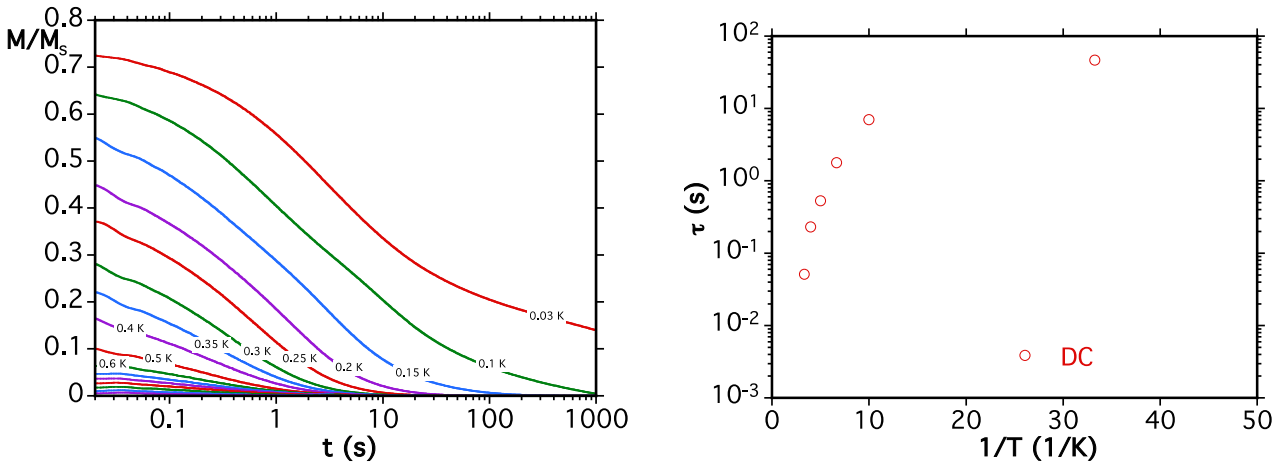

Figure S12: Magnetization decay measurements for compound **2** at the indicated temperatures (left) and relaxation time (right).

6. Thermogravimetric analysis (TGA) of compound 2

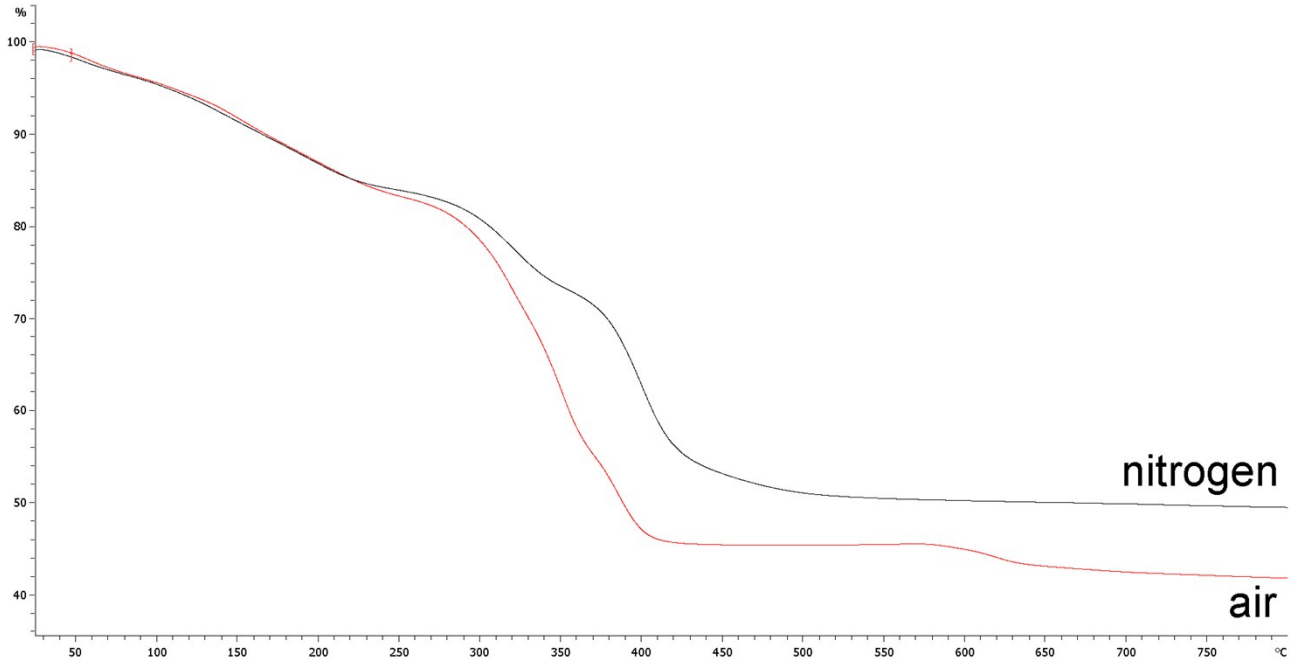

Figure S13: TGA curves of compound **2** obtained under a nitrogen atmosphere (black curve) and under air (red curve) with a heating rate of 5 K min^{-1} in the temperature range 25–800 °C by using a Mettler Toledo TGA/SDTA 851e instrument. The TGA reveals low thermal stability of compound **1** up to only 50 °C against solvent loss and degradation under N_2 and air. The complex decomposes in undefined steps.

7. References

1. CrysAlisPro, Agilent Technologies, 1.171.36.28 (release 01-02-2013 CrysAlis171 .NET).
2. G. M. Sheldrick, *Acta Cryst.* 2008, **A64**, 112.
3. K. S. Cole, R. H. Cole, *J. Chem. Phys.* 1941, **9**, 341.
4. H. Lueken, *Magnetochemie*, Teubner Verlag, Stuttgart 1999.
5. a) L. R. Piquer, E. C. Sanudo, *Dalton Trans.* 2015, **44**, 8771; b) D. N. Woodruff, R. E. P. Winpenny, R. A. Layfield, *Chem. Rev.* 2013, **113**, 5110.
6. a) W. Wernsdorfer, *Adv. Chem. Phys*. 2001, **118**, 99; b) W. Wernsdorfer, *Supercond. Sci. Technol.* 2009, **22**, 064013.